Polymer Degradation and Stability 233 (2025) 111145

Contents lists available at ScienceDirect

Polymer Degradation and Stability

journal homepage: www.journals.elsevier.com/polymer-degradation-and-stability

Thermal and flame retardant properties of recyclable disulfide based epoxy vitrimers

Valeria Berner [a,*], Arrate Huegun [b], Larissa Hammer [c], Anna Maria Cristadoro [d], Carl-Christoph Höhne [a]

[a] Fraunhofer Institute for Chemical Technology ICT, Joseph-von-Fraunhofer Str. 7, 76327 Pfinztal, Germany
[b] CIDETEC, Basque Research and Technology Alliance (BRTA), Po. Miramón 196, 20014 Donostia-San Sebastian, Spain
[c] BASF SE, Carl-Bosch-Str. 38, 67056 Ludwigshafen am Rhein, Germany
[d] BASF Polyurethanes GmbH, Elastogranstr. 60, 49448 Lemfoerde, Germany

ARTICLE INFO

Keywords:
Vitrimer
Epoxy vitrimer
Disulfide bonds
Flame retardant
Recycling

ABSTRACT

The development of flame retardant epoxy vitrimers which are suitable for use as a composite matrix material is essential for the transition to a sustainable circular economy.

In this work the thermal and flame retardant properties as well as the rheological characteristics of a common epoxy vitrimer based on DGEBA and Butanediol diglycidyl ether cured with 4-Aminophenyldisulfide (4-AFD) with different aliphatic and naphthalene-based resins as well as reactive and additive Phosphorus based flame retardants (FR) with different oxidation states were studied. The use of 4-AFD as curing agent imparts vitrimeric properties to the material and allows repairing, reprocessing and recycling. A series of epoxy vitrimers (EV) was prepared aiming to improve the flame retardant properties while maintaining the dynamism and reprocessability. The neat EV (T_g ~125 °C) showed a limited oxygen index (LOI) of 20.9 ± 0.4 %O_2 and no classification and heavy dripping in the UL-94 vertical burning test. The addition of naphthalene-based epoxy resins increased the LOI value up to 23.4 ± 0.4 %O_2, but the EV did also not reach a UL-94 classification. With 1.5 wt% of Phosphorous (P) in the EV LOI values up to 38.5 ± 0.4 %O_2 and V-0 classification with excellent self-extinguishing behavior was achieved. Especially gas phase active FRs with lower oxidation states showed better flame retardant properties in the LOI and UL-94 vertical burning tests with identical phosphorus content. In cone calorimeter test the EVs with 1.5 wt% P reduced the peak heat release rate (PHRR) up to 43 %. The addition of reactive phosphorous-based FRs did not influence the dynamism and recyclability of the material in dynamic mechanical analysis. After mechanical recycling >73 % of the mechanical strength was recovered and the flame retardant EVs do reach as well a V-0 classification in the UL-94 vertical burning test.

1. Introduction

Plastics are widely used due to their versatile and variable properties [1]. Epoxy thermosets display excellent thermal stability, adhesive, electrical and mechanical strength, as well as chemical resistance. These properties make them highly suitable for high-performance applications in the aerospace, transportation, construction, and electronics industries [2–8]. However, the permanent crosslinked molecular network of thermosets cannot be reshaped or reprocessed which leads to major challenges for recycling and their end-of-life options [9–11]. Embedding recyclability and reprocessability in thermosets presents an important step towards sustainability and a circular plastics economy [10,12].

The incorporation of dynamic covalent bonds (DCB) into a thermoset network is a powerful method for reshaping these thermoset materials through topology rearrangements allowing self-healing, stress relaxation, recyclability, reprocessability [13–16]. By an external stimulus the DCBs of these so called covalent adaptable networks (CAN) can be triggered resulting in single reversible chemical bond exchange reactions that cause molecular restructuring of the network [15,17–19]. CANs are a new class of polymeric materials closing the gap between thermoset and thermoplastic materials by exhibiting strong mechanical properties while also allowing remodeling [20]. Depending on the dynamic structure and the mechanism of bond exchange CANs are divided into two classes – associative and dissociative CANs. The dissociative

* Corresponding author.
E-mail address: valeria.berner@ict.fraunhofer.de (V. Berner).

https://doi.org/10.1016/j.polymdegradstab.2024.111145
Received 29 August 2024; Received in revised form 2 December 2024; Accepted 11 December 2024
Available online 12 December 2024

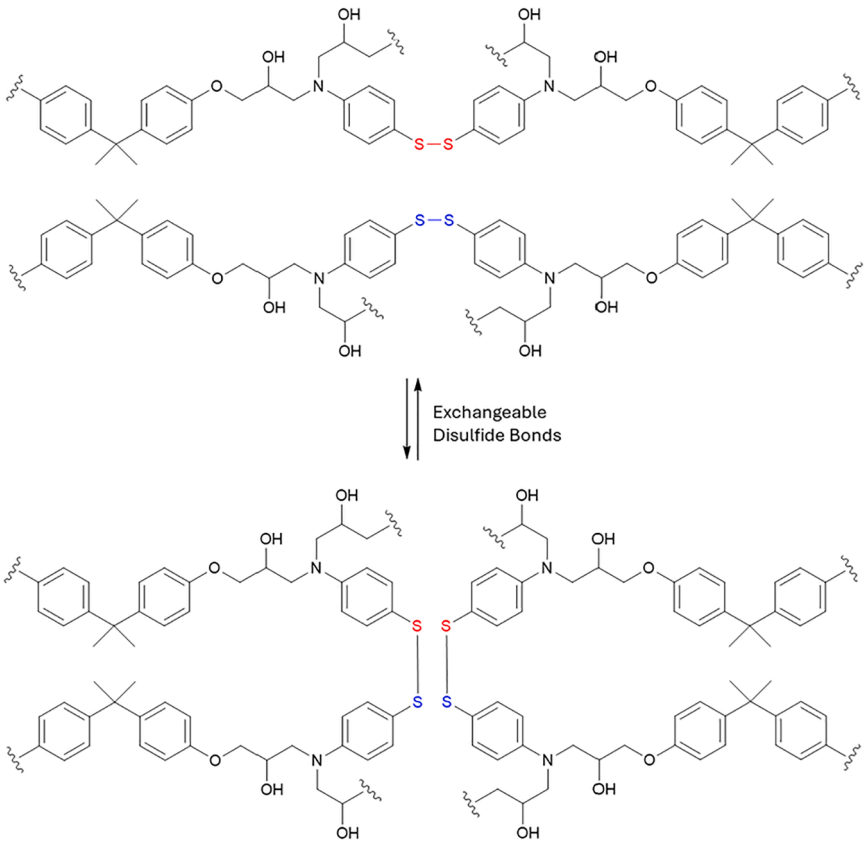

Fig. 1. Schematic structure of the desired dynamic network and the schematic exchange of the disulfide bonds.

mechanism proceeds via an elimination/addition pathway and the associative mechanism can be described via an addition/elimination pathway [16,21]. In 2011, Leibler et al. introduced the term "vitrimer" for an epoxy network with metal-catalyzed transesterification chemistry undergoing an associative mechanism [22]. The dynamic bond exchange lead to a glassy silica-like behavior [22–24]. Since then, different types of dynamic bonds were incorporated into thermoset materials. In epoxy vitrimers carboxylate transesterification [25–28], transamination [29–32], transcarbamoylation [33,34], siloxane silanol exchanges [35–37], and the exchange of disulfide bonds [38–47] are often utilized for the reprocessability.

In this work, we focused on disulfide based epoxy vitrimers which could be reprocessed, repaired and recycled [48]. MATXAIN et al. demonstrated in a theoretical study that the exchange mechanism follows a radical-mediated [2 + 1] pathway, where radical formation primarily results from the thermal dissociation of the disulfide bond [49]. In addition to mechanical recycling, chemical recycling is also possible with disulfide based vitrimers due to the chemical reduction of the disulfide bond with a reducing agent such as 2-mercaptoethanol or dithiothreitol in a suitable solvent leading to a complete dissolution of the network [41,45,48,50,51]. A schematic structure of the epoxy vitrimer network studied in this work and the schematic exchange of the disulfide bonds is presented in Fig. 1.

Beside safety, sustainability and recyclability, material properties and product requirements are essential. Flame retardant properties are mandatory for many plastic application, especially for epoxy thermosets in the transportation, building and construction sector as well as for an application in electronics [52–54].

Flame retardant additives have different mode of actions, they can eighter act in the gas or in the condensed phase by interrupting the combustion process during heating, pyrolysis, ignition or flame propagation [52]. Phosphorus compounds are known as highly effective flame retardants for a variety of plastics [55]. Phosphorus based flame retardants can act in the condensed phase by promoting char, intumescence or inorganic glass formation. In the gas phase they can act by flame inhibition [55–57]. The oxidation state of the phosphorus[1] and the chemical environment of the phosphorus has an influence on the mode of action. Phosphorus compounds with a low oxidation state, such as phosphine oxides, have a higher activity in the gas phase whereas phosphorus based flame retardants with a higher oxidation state, such as phosphates, exhibit a higher activity in the condensed phase [53,58]. However, frequently both flame retardant mode of actions are present in phosphorous modified flame retardant polymers [58–60]. Often a combination of different types of flame retardants which support each other synergistically in their flame retardancy is applied for plastics [61]. A synergistic effect with phosphorus FRs has also been observed for sulfides and disulfides with activity in the gas phase as radical scavengers and in the condensed phase by drip promotion [61–63].

Since flame retardancy and recyclability are rarely achieved

[1] The theoretical oxidation state of phosphorus in an organo phosphorus compound, usually V and III depending on the tautomeric structure possible, does not change when an oxygen phosphorus bond is replaced by a carbon phosphorus bond due to the lower electronegativity of phosphorus compared to carbon and oxygen. However, since it is a common designation in the flame retardant literature [55–57] to distinguish organo phosphorus species, we use the term "oxidation state of P" to indicate the chemical nature of the compound class, which is "-I" for phosphine oxide; "+I" for phosphinate; "+III" for phosponate; and "+V" for phosphate. In the flame retardant area, correlations are found between the mode of action and the number of phosphorus-oxygen bonds vs. phosphorus-carbon bonds, assumed to be cause by the differences in bond energies. However, it is emphasized that the "oxidation state of P" mentioned in this paper is not an indication of the actual electron density at the phosphorus atom of these compounds. It is an indication of the number of phosphorus-oxygen bonds and an indication the assumed preferred flame retardant mode of action.

Table 1
Formulations of manufactured and tested EVs with the oxidation state (OS) of the FR compound and calculated Phosphorous (P_{cal}) and Sulfur (S_{cal}) content.

Sample	Aliphatic resin or FR	Chemical substance	OS of P	Araldite® LY 1564 / wt%	4-AFD / wt%	Aliphatic resin / wt%	FR / wt%	P_{cal} /wt%	S_{cal} / wt%
EV-0	–	DGEBA + Butanediol-diglycidylether	–	69.4	30.6	–	–	–	7.9
EV-1	DY-D	Butanediol-diglycidylether	–	46.9	33.1	20.1	–	–	8.5
EV-2	CY184	Diglycidyl-1,2-cyclohexane dicarboxylate	–	48.3	31.1	20.7	–	–	8.0
EV-3	HP 4032D	1,6-Bis(2,3-epoxypropoxy)naphthalene	–	47.7	31.8	20.5	–	–	8.2
EV-4	MPO	1-Methylphospholane-1-oxide	*-I*	65.7	29.0	–	5.3	1.4	7.5
EV-5	RP 6500	Red phosphorous microencapsulated in epoxy resin carrier	*0*	67.2	29.7	–	3.1	1.4	7.6
EV-6	OP 930	Aluminium diethyl phosphinate	*+I*	65.2	28.8	–	6.0	1.4	7.4
EV-7	Polyphlox® 3742	9,10-Dihydro-9-oxa-10-phosphaphenanthrene-10-oxide (DOPO) modified epoxidized novolac	*+I*	37.9	24.2	–	37.9	1.5	6.2
EV-8	EP 360	Phosphorus modified epoxy resin	*+I/ +III*	51.0	25.9	–	23.1	1.5	6.7
EV-9	PCO 900	3,9-dimethyl-2,4,8,10-tetraoxa-3,9-diphosphaspiro [5.5]undecane 3,9-dioxide	*+III*	65.3	28.8	–	5.9	1.4	7.1
EV-10	AP 423	Ammonium polyphosphate	*+V*	66.2	29.3	–	4.5	1.4	7.5

simultaneously, the addition of flame retardants for the epoxy vitrimer based on disulfide bonds is needed.

There are a few approaches in which phosphorus-based species were synthesized for incorporation in vitrimers and enhanced flame retardant properties were achieved [54,64–70].

However, these flame retardant investigations are performed on chemical lab-scale using newly developed compounds, which leads to limited availability and hampers large-scale applications.

In this work, we developed different epoxy vitrimer formulations with commercially available aliphatic, aromatic and naphthalene-based resins as well as commercially available phosphorus based flame retardants. We investigated the influence of the ratio of aliphatic and aromatic chains and the influence of the oxidation states and chemical environment of the phosphorous compound to identify whether there is a preferred compound and oxidation state to achieve outstanding flame retardant properties in epoxy vitrimers containing disulfide bonds.

2. Materials and methods

2.1. Materials

The DGEBA based bifunctional epoxy resin Araldite® LY 1564 (epoxy equivalent weight (EEW 161 – 173 g•eq^{-1}), and the aliphatic bifunctional epoxy resin Araldite® DY-D (EEW 117 – 125 g•eq^{-1}), and Araldite® CY 184 (EEW 144 – 172 g•eq^{-1}) were purchased from Huntsman. The naphthalene-based epoxy resin Epiclon® HP-4032D (EEW 136 – 148 g•eq^{-1}) was purchased from DIC Corporation. The hardener 4-Aminphenyldisulfide (4-AFD) was procured from Molekula Group. The Flame retardants 1-Methylphospholene-1-oxide (MPO), Exolit® RP6500, Exolit® OP 930, Exolit® AP 423 and Exolit® EP 360 (EEW 470 – 650 g•mol^{-1}) were obtained from Clariant. Polyphlox® 3742 (EEW 375 g•eq^{-1}) was received from Struktol Schill + Seilacher. The Phosphonate Aflammit® PCO 900 were obtained from THOR.

2.2. Preparation of resin plates

The flame retardants and aliphatic resins were premixed with the Araldite® LY 1564 for 15 min at 120 °C, 500 rpm and degassed using a dissolver DISPERMAT from VMA-Getzmann GmbH. The phosphorus-content of the flame-retardant-resin mixture was about 2 wt.%. The aliphatic resins have been premixed with Araldite LY 1564 with a content of 30 wt.%. The hardener itself was also heated up to 80 °C, stirred and degassed for 5 min. After the addition of the hardener to the resin, the mixture was stirred for 5 min at 120 °C, 2000 rpm degassed using the dissolver DISPERMAT from VMA-Getzmann GmbH. The liquid mixture was then poured in an aluminum mold (150 × 180 × 4 mm^3) or a glass mold (100 × 100 × 1 mm^3) lined with teflon foil (0.7 mm, Hightechflon GmbH & Co. KG) and cured an oven (Binder Solid.Line™ FD-S) at gradually increasing temperatures (120 °C for 2 h and 150 °C for 2 h) to obtain the cured EV samples [66].

The cured samples were cut into specimen for fire testing, stress-relaxation experiments using a band saw Micromot MBS 240 from PROXXON. The detailed formulations are listed in Table 1.

2.3. Reprocessing and recycling of EV

The cured EV samples were cut in small pieces (approx. 20 × 50 × 4 mm^3) with a band saw Micromot MBS 240 from PROXXON followed by milling using a cutting mill with 1 mm sieve insert from Hosokawa Alpine AG). The EV powder was transferred into a steel mold (130 × 130 × 2 mm^3) and hot pressed with a lab press from Collin under 200 °C with gradually increased pressures: 2 bar for 10 min, 50 bar for 10 min, 200 bar for 5 min, Cooling to 60 °C. The mold was removed when the temperatures were below the T_g (approx. below 100 °C) to receive the reprocessed samples. Specimens for mechanical tensile tests and UL-94 vertical burning tests were prepared using a band saw Micromot MBS 240 from PROXXON.

2.4. Characterization methods

2.4.1. Fourier transform infrared spectroscopy (FTIR)

For FTIR a Nicolet iS50 from Thermo Scientific with attenuated total reflectance (ATR) was used and cured EV samples were measured from 650 cm^{-1} to 4000 cm^{-1}.

2.4.2. Differential scanning calorimetry (DSC)

DSC measurements were performed using a DSC 1 from Mettler Toledo. The samples were measured in an aluminum crucible with a hole in the lid between 25 – 250 °C at a heating rate of 10 K•min^{-1} under nitrogen atmosphere. The weight of the sample was 10 mg. A double determination was carried out for validation, but only one measurement is shown in this work. The glass transition temperature (T_g) was determined using the "tangent method." This involves identifying the intersection of tangents drawn on the baseline and the low-temperature peak side of the curve. The curing enthalpy of reactive EV samples is proportional to the area of the exothermic curing peak, the onset corresponds to the temperature value where the energy release started. T_g values and curing enthalpies shown here were obtained from the first heating cycle.

2.4.3. Thermogravimetric analysis (TGA)

TGA measurements were carried out with a Netzsch TG 209 F1 Iris measuring instrument under nitrogen atmosphere with a heating rate of 10 K•min^{-1} between 25 – 1000 °C in an Al_2O_3 crucible. The weight of the

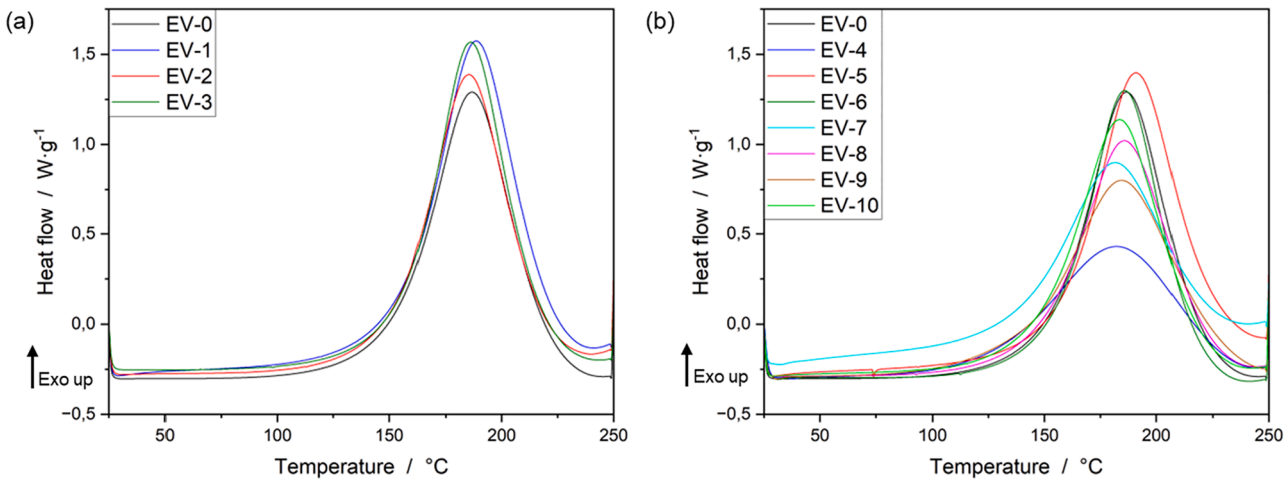

Fig. 2. First heating cycle DSC curves of the exothermic curing reaction of (a) the EVs with other epoxy resins and (b) the EVs with FRs.

sample was 10 mg. A double determination was carried out for validation, but only one measurement is shown in this work.

2.4.4. Thermogravimeter coupled with mass spectrometer (TG-MS)

The decomposition products of the EVs were detected with TG-MS by coupling the TG 209 F1 Iris measuring device from Netzsch with the QMS 403 C Aeolos mass spectrometer from Netzsch. The measurements were carried out under nitrogen atmosphere with a heating rate of 10 K•min^{-1} between 25 – 1000 °C in an Al_2O_3 crucible. The weight of the sample was 10 mg. The mass spectrometer recorded values in the range of *m/z*: 10 – 120.

2.4.5. Limiting oxygen index (LOI)

The LOI was determined on an oxygen index module from FIRE in accordance to DIN EN ISO 4589–2:1999 + A1:2006 using type III test specimens (dimensions: 80 × 10 × 4 mm^3).

2.4.6. UL-94 vertical burning test

The UL-94 vertical burning test was performed in a test chamber from WAZAU according to ASTM-D3801 with specimen with 125 × 13 × 4 mm^3.

2.4.7. Cone calorimeter test (CCT)

CCTs were carried out on a test device from WAZAU according to ISO 5660–1 with a sample size of 100 × 100 × 4 mm^3 and 100 × 100 × 2 mm^3 at a heat flux of 50 kW•m^{-2}.

2.4.8. Stress-relaxation tests

The tensile stress-relaxation experiments have been performed on a TA INSTRUMENTS DMA Q800 equipment controlled by TA Universal Analysis software to evaluate the dynamism of each material. For the stress-relaxation measurements samples with 20 × 6 × 1 – 1.5 mm^3 were tested. Samples were initially preloaded at a force of 10^{-3} N to assure straightness and heated to testing temperature followed by 5 min of tempering. Once the required temperature was reached, the specimens were stretched with a strain of 1 % during the test. The decrease in stress over time at each temperature was recorded. The normalized stress relaxation modulus (G/G_0) was calculated and plotted against time.

2.4.9. Tensile tests

Tensile tests have been carried out according to ISO 527–2ASTM D638, using 1 – 1.5 mm thick V-type dog bones specimens. These mechanical tests have been performed on an Instron 3365, equipped with a 5 kN load cell, at a speed of 1 mm•min^{-1} at dry conditions.

Table 2
Curing enthalpies and curing temperatures of the EV-0, EV-1, EV-2 and EV-3.

Sample	Curing enthalpy / J•g^{-1}	T_{Onset} / °C	T_{Peak} / °C
EV-0	430	151	188
EV-1	453	155	189
EV-2	410	152	189
EV-3	446	155	187

3. Results and discussion

3.1. Curing of the epoxy vitrimers

The curing behavior of the vitrimers with other epoxy resins and flame retardants were studied with DSC and the complete curing was verified with FTIR.

Aliphatic and naphthalene-based epoxy resins were added with 30 wt% to the epoxy resin Araldite® LY1564 to analyze the impact of the ratio of aromatic and aliphatic chains. Fig. 2(a) presents the DSC curves of the exothermic curing of the epoxy vitrimers. The reference EV-0 begins to cure at 151 °C and exhibits a peak of the curing reaction at 188 °C (Table 2). The addition of aliphatic and naphthalene-based epoxy resins do not influence the starting temperature of the curing reaction or the peak temperature of the curing reaction. The temperature of the curing reaction does therefore not depend on the structure and flexibility of the epoxy resin. It is reported that aliphatic amines are more reactive than aromatic amines towards epoxy groups. Accordingly, the onset temperatures with aliphatic amines are lower than those with aromatic amines [71]. In this work an aromatic amine was used for curing, explaining the higher temperatures needed for the curing reaction.

The curing enthalpy for EV-0 is 430 J•g^{-1} and increased for EV-1 and EV-3. Due to a lower EEW of 117 – 125 g•eq^{-1} for Araldite® DY-D and 136 – 148 g•eq^{-1} for Epiclon® HP-4032D the density of epoxy groups per gram reactive sample is higher, resulting in a higher curing enthalpy. For EV-2 the curing enthalpy decreased even though the EEW is similar to EV-0. It is assumed that the cyclohexane fragment restricts chain flexibility, thereby affecting chain mobility during the curing process.

Phosphoros based flame retardants seem to be a promising solution to lower the flammability of this disulfide based epoxy vitrimer. Seven different phosphorous-based flame retardants (see Table 1) were selected based on their oxidation state, the chemical environment of the phosphorous and the presence of free epoxy groups for covalent incorporation to investigate the influence thereof on the flame retardancy. The aim is to determine a preferred oxidation state for the epoxy vitrimer.

Table 3
Curing enthalpies and curing temperatures of EVs with phosphorous-based FRs.

Sample	OS of P	Curing enthalpy / J•g^{-1}	T_{Onset} / °C	T_{Peak} / °C
EV-4	*-I*	270	126	182
EV-5	*0*	413	157	182
EV-6	*+I*	404	150	185
EV-7	*+I*	303	138	182
EV-8	*+I/+III*	377	147	186
EV-9	*+III*	373	139	185
EV-10	*+V*	385	146	183

For the flame retardant testing it is important that the phosphorous compound is successfully integrated into the vitrimer. Fig. 2(b) shows the DSC curves of the exothermic curing reaction of the epoxy vitrimers with different flame retardants. Table 3 summarizes the curing properties.

The addition of flame retardants led to a decrease in the curing enthalpy and thus a lower heat release during curing process. Mixing the epoxy resin with the phosphorus FR increases the EEW resulting in a lower amount of free epoxy groups per gram reactive sample which explains the reduced curing enthalpy. The lower heat release correlates with the higher EEW for all EV samples except for EV-4. For EV-4, the resulting mix EEW increases only slightly, but the heat release decreases by 37 %, which cannot only be explained by fewer epoxy groups. It is assumed that the curing reaction is disturbed by MPO. However, the IR of EV-4 gives no indication that no complete curing reaction takes place, the bands of the epoxy groups disappear (see supporting information Fig S1) as well as those of the other samples (see Fig. 3).

Furthermore, for EV-4 the onset temperature of the curing reaction decreased by 25 °C. EV-7, EV-8, EV-9 and EV-10 show also decreased onset temperatures by 5 – 13 °C. EV-5 and EV-6 show with 157 °C and 150 °C similar onset temperatures as EV-0. The peak temperature of the curing reaction however remains around 185 °C. The phosphorus flame retardant thus leads to an initiation of curing at lower temperatures; although, the main step of the reaction is not affected. An influence of phosphorus flame retardants on the curing behavior was also observed in other studies [72–74]. It is possible that the phosphorous-based flame retardants exhibit a catalytic effect leading to decreased onset temperatures of the curing reaction as it is known for e.g. tertiary amines and phosphines [72,73,75,76].

To confirm the reaction between the 4-AFD and the epoxy resin FTIR analysis was performed. The spectra of the uncured epoxy resin Araldite® LY 1564, the cured EV-0, the cured EV-1 containing 20 wt% aliphatic resin Araldite® DY-D and EV-8 containing the reactive phosphorous-based FR Exolit® EP 360 are presented in Fig. 3.

The FTIR spectra of the other EVs are given in the supporting information Fig S1.

The curing of the EV should become visible through the disappearance of the characteristic absorption peaks for epoxy groups between 3075 – 3040 cm^{-1} for the asymmetric C—H stretching vibration of the CH_2 group of the oxirane ring and between 965 – 875 cm^{-1} for the asymmetric deformation vibration of the oxirane ring [77–79]. In Fig. 3 the peaks at 910 cm^{-1} and 3050 cm^{-1} disappear after curing indication a complete conversion of the epoxy groups. Besides the disappearance of the epoxy group vibration, the formation of thy hydroxyl groups due to the curing reaction can be observed by the hydroxyl stretching vibrations at 3400 cm^{-1}. Furthermore, the addition of 20 wt% aliphatic epoxy resin Araldite® DY-D in EV-1 led to a higher intensity of the peak at 2865 cm^{-1} confirming a higher content of CH_2 groups. For EV-8, a peak can be observed at 1090 cm^{-1}, which could indicate the symmetrical $P=O$ stretching vibration of the added phosphorus based reactive flame retardant Exolit® EP 360. However, the overall low amount of phosphorus in the sample of 1.5 wt% P could also lead to an overlapping of the characteristic vibrations ($P=O$ stretching vibration between 1350 cm^{-1} and 1150 cm^{-1} and asymmetric stretching vibration of P-O-C between 1050 cm^{-1} and 970 cm^{-1} [77]) of phosphorous compounds with vibrations of the epoxy vitrimer matrix.

3.2. Thermal properties and flame retardancy

The glass transition temperature T_g is a crucial parameter of epoxy vitrimers and affects their application. The T_g was determined with DSC and the curves of the EVs with other epoxy resins and phosphorous-based flame retardant are shown in the supporting information Fig S2.

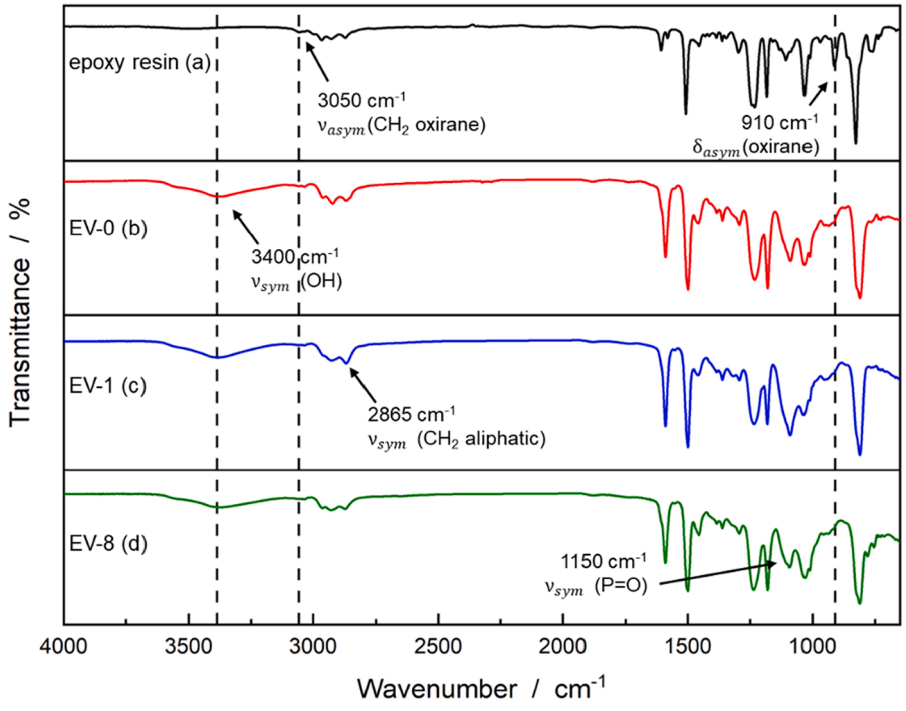

Fig. 3. FTIR spectra of the (a) uncured epoxy resin (Araldite® LY 1564), (b) EV-0, (c) EV-1, (d) EV-8.

Table 4
Thermal analysis results from TGA and DSC and flame retardant properties of EVs without flame retardants. T_{dMax} is the temperature with the biggest mass loss.

Sample	T_g / °C	TGA			LOI / % O_2	UL-94
		$T_{2\ \%\ mass\ loss}$ / °C	T_{dMax} / °C	Residue (1000 °C) / %		
EV-0	125	274	331	13.6	20.9 ± 0.4	n.c.
EV-1	100	263	337	12.6	21.0 ± 0.4	n.c.
EV-2	115	262	326	11.8	21.1 ± 0.5	n.c.
EV-3	139	275	333	16	23.4 ± 0.4	n.c.

Table 5
Thermal analysis results from TGA and DSC and flame retardant properties of EVs with FRs. T_{dMax} = temperature of highest mass loss.

Sample	OS of P	T_g / °C	TGA			LOI / %O_2	UL-94
			$T_{2\ \%\ mass\ loss}$ / °C	T_{dMax} / °C	Residue (1000 °C) / %		
EV-4	*-I*	118	237	290	14.3	31.3 ± 0.5	V-1
EV-5	*0*	120	272	325	17.2	27.9 ± 0.4	V-1
EV-6	*+I*	125 / 171	271	328	18.5	29.6 ± 0.3	V-0
EV-7	*+I*	116	277	326	22.4	29.0 ± 0.4	V-0
EV-8	*+I/ +III*	113	273	332	19.5	38.5 ± 0.4	V-0
EV-9	*+III*	122	265	304	23.1	31.5 ± 0.4	V-1
EV-10	*+V*	125	268	292	24.5	23.8 ± 0.5	n.c.

EV-0 shows a T_g of 125 °C (see Table 4). Aliphatic chain segments decreased the T_g by 25 °C for EV-1 and 10 °C for EV-2 due to a higher rotation flexibility of the added aliphatic chains. EV-3 shows an increase of the T_g up to 139 °C due to the limited rotation flexibility of the naphthalene segments.

Typically, the use of flame retardants has a significant impact on the glass transition temperature of thermosets composites and thereby affecting their overall applicability [80]. The T_g of the EVs with FRs are slightly lower than the one of the neat EV-0 (Table 5 and supporting information Fig S2 (b)) and remain the same for EV-6 and EV-10. The highest reduction for the additive flame retardants is observed for EV-4 with a T_g of 118 °C. Both reactive flame retardants lead to a T_g reduction of 9 – 12 °C to 116 °C for EV-7 and 113 °C for EV-8. Many phosphorus-based flame retardants exhibit plasticizing effects in epoxy thermosets [80–82]. Furthermore, the presence of the FRs could interfere with the curing reaction leading to a lower crosslink density. Due to the low amounts of flame retardant of about 1.5 wt% of phosphorus these effects are only weakly apparent in the EVs of this study.

All EVs show a single transition except for EV-6 which shows a second transition at 171 °C. A micro phase separating effect caused by the non-reactive flame retardant particles is assumed to be the cause of this effect. Other studies also observed two transition temperatures by having microphase separation of block-copolymer based vitrimers [83].

Thermal stability is a key benefit of epoxy resins in comparison to thermoplastics and allow use in higher temperature applications. However, vitrimers can be reprocessed induced by temperature. The combination of thermal stability and processibility is therefore of major importance for a later application of vitrimers. This epoxy vitrimer studied here is reprocessed by the disulfide exchange taking place above T_g. The maximum reprocessing temperature was determined using TGA onset temperature of the mass loss. The glass transition, TGA results of EV-0 and the different combinations with aliphatic and naphthalene-based resins are summarized in Table 4 and TGA and DTG curves are shown in Fig. 4.

EV-0 shows thermal stability upon 274 °C (2 % mass loss) and a residue of 13.6 % at 1000 °C. The combinations with aliphatic resin EV-1 and EV-2 leads to a about 12 °C lower onset temperature of about 262 °C due to the higher flexibility of the aliphatic chain segments and reduced intermolecular interactions. The naphthalene-based resin combination EV-3 shows an equal thermal stability of 275 °C in comparison to EV-0. The same trend can also be observed for the residue at 1000 °C. The residue of EV-0 is 13.6 %. The residue decreased for EV-1 and EV-2 to 12.6 % and 11.8 % due to a reduced amount of aromatic structures which could contribute to the char formation. In addition, aliphatic fragments are more volatile and can more easily transition into the gas phase during decomposition. The naphthalene-based resin combination EV-3 shows an increased residue of 16.0 % due to an increased char formation supported by the naphthalene structures. All four EVs exhibit a single-stage thermal decomposition step with the highest mass loss around 331 °C. However, the DTG curves show two peak maxima, indicating an overlap of two decomposition steps. The initial step in the thermal decomposition of epoxy resins involves the dehydration of secondary hydroxyl groups. This is followed by the release of low molecular weight volatile compounds through cleavage and cyclization

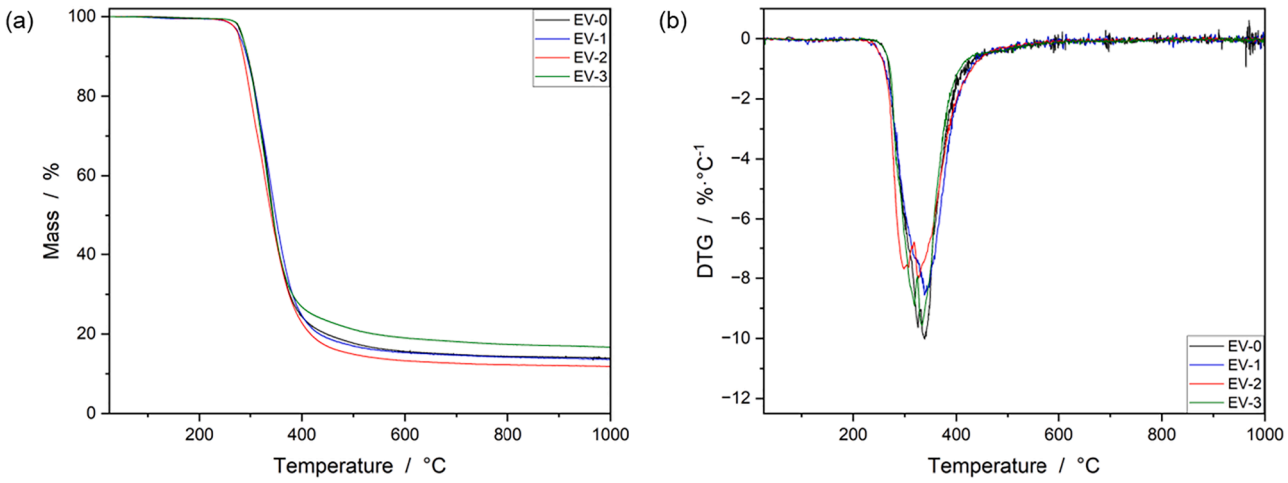

Fig. 4. TG (a) and DTG (b) curves of EV-0, EV-1, EV-2 and EV-3.

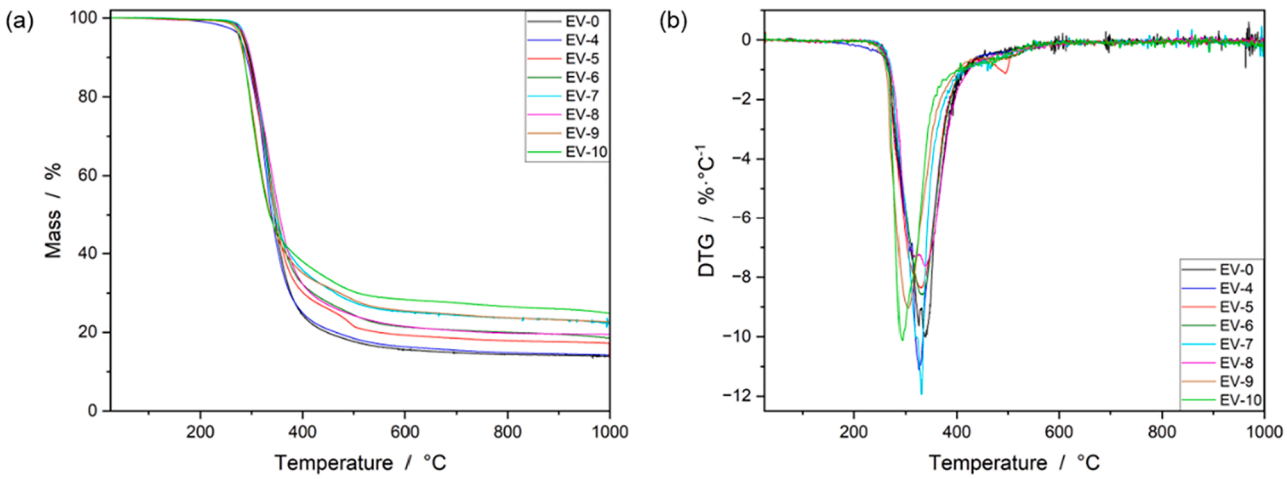

Fig. 5. TG (a) and DTG (b) curves of the EVs with FRs.

reactions. These decomposition processes likely overlap, resulting in a decomposition curve that displays two distinct points with the maximum mass loss corresponding to each step [84,85].

The flammability of the four EVs was investigated by LOI tests and UL-94 vertical burning tests to study the influence of the aliphatic and aromatic structures on the flammability of the EV. The results are summarized in Table 4. EV-0 showed a LOI of 20.9 ± 0.4 %O_2 and did not reach a UL-94 classification. Other epoxy vitrimers without flame retardants and sulfur species like DGEBA cured with citric acid shows a LOI value of 18 %O_2 [54]. Moreover, an epoxy thermoset based on DGEBA cured with Diamino diphenylmethane shows and LOI value of 19 %O_2 [86]. This indicates, however weak, a flame retardant effect of the disulfide structures of the EV studied here as flame retardant by the release of thiyl radicals into the gas phase [63].

The combination with aliphatic resins did neither improve nor worsen flammability measured by LOI test. LOI of about 21 %O_2 are observed for EV-1 and EV-2. However, the naphthalene-based resin combination EV-3 shows an improved LOI value of 23.4 ± 0.4 %O_2. The increased tendency of char formation already observed during the TGA measurements is assumed to be the cause of this reduced flammability. However, none of the four EVs reaches an UL-94 classification. This clearly indicates the need of flame retardant solutions for this type of EV.

The thermal stability and the flammability were investigated for the EVs containing the selected phosphorus based FRs. The TG (a) and DTG (b) curves are shown in Fig. 5 and the corresponding data as well as the LOI values and UL-94 classifications are presented in Table 5.

The thermal decomposition of the EVs containing flame retardant proceeds through a main decomposition step between 230 °C to 500 °C.

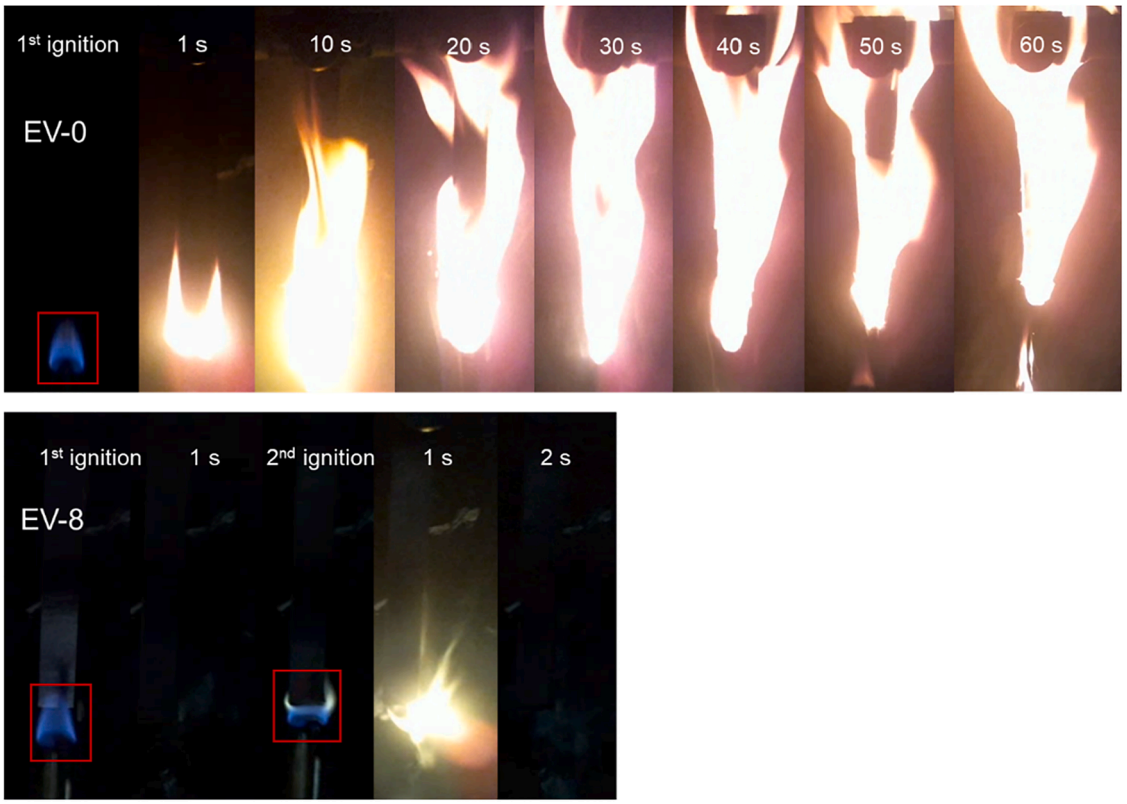

Fig. 6. Illustration of the flame retardant performance of the flame retardant free EV-0 in comparison to the flame retardant EV-8 during UL-94 test.

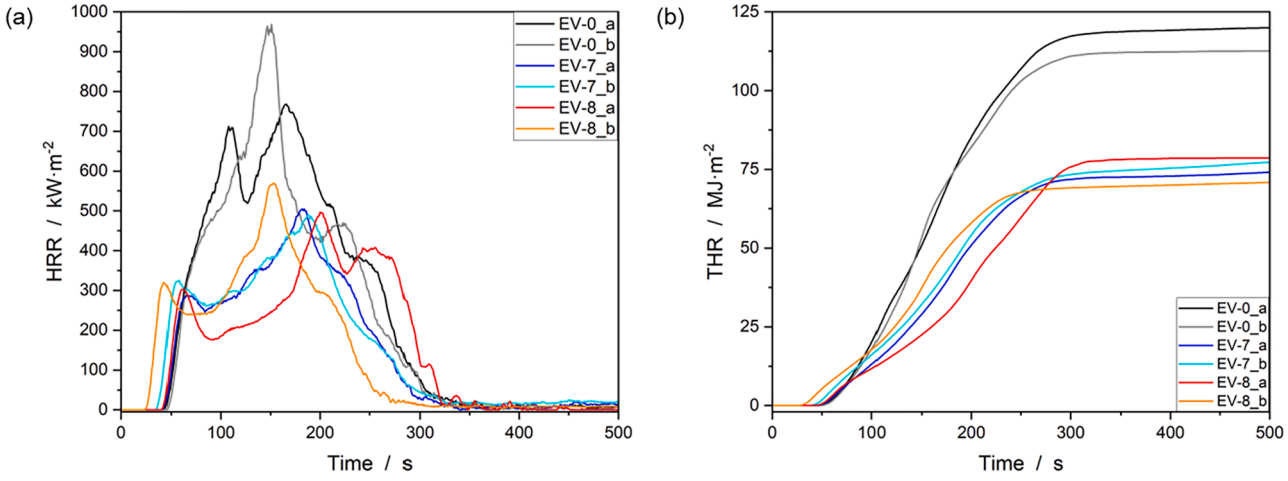

Fig. 7. Cone calorimeter curves of (a) HRR and (b) THR of EV-0, EV-7 and EV-8.

EV-4, EV-9 and EV-10 lower $T_{mass\ loss\ 2\ \%}$ by up to 37 °C to a range of 237 – 268 °C. EV-5, EV-6, EV-7, and EV-8 shows similar decomposition temperatures as EV-0. A lower onset temperature of the thermal decomposition caused by phosphorous-based flame retardants is frequently described in the literature [74,84,87–89]. The phosphorus-organic compounds lower the activation energy for thermal decomposition due to the lower thermal stability of the P–O bonds [88,89]. For the EVs containing flame retardant, the DTG curves show a weak shoulder at 500 °C indicating a minor mass loss step. For EV-5 the phenomenon is especially noticeable. It is assumed that phosphorus based flame retardants form a char layer, but this layer may not be stable. Parts of it can transition into the gas phase as soot, leading to further mass loss.

The residue at 1000 °C of the EVs is increased with increasing oxidation state of the phosphorous indicating an enhanced activity of these compounds in the condensed phase. For EV-4 the residue increased by only 0.7 %, indicating that MPO does not lead to any significant char formation of the vitrimer but likely exhibits activity in the gas phase. For EV-5, EV-6, EV-7, EV-8 a higher residue was observed suggesting char formation during the decomposition. EV-9 and EV-10 exhibit residues > 23 % indicating a strong activity in the condensed phase of the phosphonate and the APP.

LOI and UL-94 were performed on all EVs to investigate the flammability with the different oxidation states of the phosphorus. For all EVs containing phosphorous flame retardant the LOI was improved in comparison to EV-0 LOI of 20.9 $\%O_2$, see Table 5 and supporting information Fig S3. EV-10 showed the lowest LOI increase up to 23.8 $\%O_2$. The highest LOI increase is observed for EV-8 with an increase of about 18 $\%O_2$ to a LOI of 38.5 $\%O_2$.

In UL-94 vertical burning test EV-10 did not reach a classification but the addition of APP did stop the dripping. EV-4, EV-5 and EV-9 reach a V-1 classification and for EV-6, EV-7 and EV-8 a V-0 classification was reached.

In Fig. 6 are pictures of the UL-94 test of EV-0 and EV8 presented. EV-0 showed after burning times of > 60 s and burning dripping which was associated with the ignition of the cotton. Additionally, the mass loss becomes apparent due to the shrinking test specimens. The flame retardant EV-8 extinguishes immediately after the first 10 s ignition phase and show a very short 1 s afterburn time after the second 10 s ignition phase. No burning dripping is observed.

These results indicated that FRs with a high activity in the condensed phase such as APP are less suitable for the vitrimer investigated in this work. Flame retardants with a higher activity in the gas phase especially phosphinates (OS +*I*) show a strong reduction of the flammability of the EV even at low levels of 1.5 wt% P.

Beside the outstanding flame retardant effect of the reactive flame retardants Polyphlox® 3742 and Exolit® EP 360 EV-7 and EV-8 offer the advantage that the phosphorus compound is covalently bond to the vitrimer network which prevents leaching during the product life time [52]. As EV-7 and EV-8 achieved the best performance in flammability tests and the FRs are covalently bond, both materials were used for further investigations.

Table 6
Cone calorimeter data of EV-0, EV-7 and EV-8.

Parameter	EV-0	EV-7	EV-8
Residue / %	4.7 ± 2.7	6.4 ± 3.2	0.4 ± 0.6
TTI / s	43.5 ± 1.0	38.5 ± 6.4	33.5 ± 10.6
Burning time / s	553 ± 314.0	355 ± 56.6	1709.0 ± 11.3
PHRR / $kW•m^{-2}$	868.3 ± 142.9	497.3 ± 10.4	533.1 ± 51.5
THR / $MJ•m^{-2}$	116.8 ± 5.4	82.3 ± 4.5	77.0 ± 5.0
FIGRA / $kW•m^{-2}•s^{-1}$	5.5 ± 1.3	2.7 ± 0.1	3.1 ± 0.9
MAHRE / $kW•m^{-2.}$	424.8 ± 11.9	273.1 ± 7.4	272.4 ± 24.6
TSR / $m^2•m^{-2}$	4567.5 ± 225.8	4937.0 ± 347.8	5722.5 ± 585.2

Cone calorimeter tests were performed to analyze the combustion behavior, heat release rate (HRR) and total heat release (THR). Two samples of EV-0, EV-7 and EV-8 were tested. The HRR and THR curves are shown in Fig. 7 and the results are listed in Table 6.

For EV-0 the PHRR and THR is about 868 $kW•m^{-2}$ and 117 $MJ•m^{-2}$. By the addition of the two reactive flame retardants the PHRR is reduced up to 43 % for EV-7 and 39 % for EV-8 and the THR is reduced by 30 % for EV-7 and 34 % for EV-8. The maximum average rate of heat emission (MAHRE) provides an indicator of the potential hazard posed by actual fire scenarios [90]. For EV-0 a MAHRE value of 425 $kW•m^{-2}$ is calculated while EV-7 and EV-8 show strongly reduced MAHRE values of 273 $kW•m^{-2}$ and 272 $kW•m^{-2}$.

For EV-0, a residue of 4.7 % was observed which increased for EV-7 to 6.4 % indicating also a slight activity in the condensed phase by promotion of char formation. This observation is in line with observations of other studies [91,92], indicating a dual flame retardant mechanism in the gas phase as well as in the condensed phase for this type of DOPO modified epoxidized novolac resins. In contrast, for EV-8 a residue of 0.4 % is observed, indicating a strong gas phase activity of this flame retardant. The strong gas phase activity of both flame retardants leads to an increase of the total smoke release (TSR). In comparison with EV-0, the TSR increases from 4568 $m^2•m^{-2}$ to 4937 $m2•m^{-2}$ for EV-7 and 5723 $m^2•m^{-2}$ for EV-8. As combustion processes in the gas phase are disrupted by the flame retardants, incomplete combustion leads to an increasing smoke formation.

To obtain more insights regarding the present flame retardant mechanism of EV-7 and EV-8 the released volatile products formed

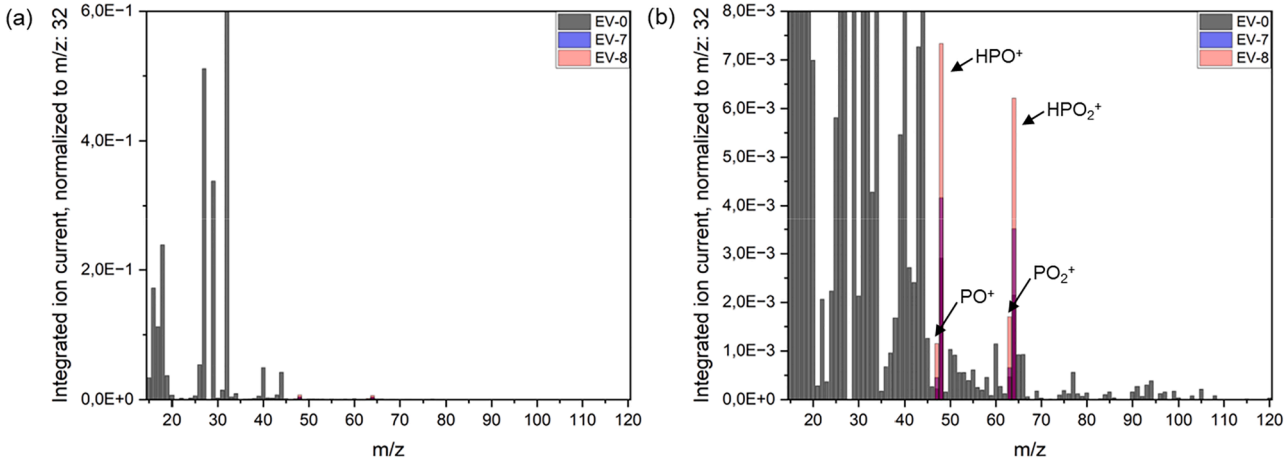

Fig. 8. Integrated normalized ion current of TG-MS of EV-0, EV-7 and EV-8 between 15 and 120 *m/z*, (b) shows (a) with a magnification of the y-axis between 0 and 8•10^{-3}. The signals at $m/z = 14$ and $m/z = 28$ are related to the carrier gas nitrogen and not shown in the figures.

during the decomposition process were analyzed with TG-MS up to a *m/z* (mass per charge) of 120. The signals at each *m/z* were integrated and normalized to the signal at $m/z = 32$ referring to the release of sulfur, see Fig. 8. During the decomposition of EV-0, mass spectrometry reveals the presence of indicators for C_1 fragments (*m/z*: 12 (C^+), 13 (CH^+), 14 (CH_2^+) 15 (CH_3^+), 16 (CH_4^+)), C_2 fragments (*m/z*: 26 ($C_2H_2^+$), 27 ($C_2H_3^+$), 29 ($C_2H_5^+$), 44 ($C_2H_4O^+$)), as well as C_3 fragments (*m/z*: 41 ($C_3H_5^+$), 42 ($C_3H_6^+$), 43 ($C_3H_7^+$)) and C_4 fragments (*m/z*: 52 ($C_4H_4^+$), 53 ($C_4H_5^+$), 54 ($C_4H_6^+$), 55 ($C_4H_7^+$), 56 ($C_4H_8^+$/CH_2CHOCH^+), 57 ($C_4H_9^+$), 58 ($CH_2CHCHOH^+$)). Additionally, S_1 fragments associated with disulfide bonds (*m/z*: 32 (S^+), 33 (HS^+), 34 (H_2S^+), 44 (CS^+), 48 (SO^+), 64 (SO_2^+)) and S_2 fragments (*m/z*: 64 (S_2^+), 65 (S_2H^+), 66 (S_2H2^+)) are detected. Aromatic fragments (*m/z*: 76 ($C_6H_4^+$), 77 ($C_6H_5^+$), 78 ($C_6H_6^+$), 93 ($C_6H_5NH_2^+$/$C_6H_5O^+$), 94 ($C_6H_5NH_3^+$/$C_6H_5OH^+$)) are also observed. Water (*m/z*: 17 (OH^+), 18 (H_2O^+), 19 (H_3O^+)) and ammonia-related compounds (*m/z*: 16 (NH_2^+), 17 (NH_3^+), 18 (NH_4^+)) are detected as well. It should be noted that larger fragments may condense in the transfer line (at 280 °C) and thus may not be captured by the mass spectrometer. Additionally, it is possible that substituted aromatic fragments with $m/z > 120$ could form and enter the gas phase but are not detected by the mass spectrometer. Otherwise, the aromatic fragments are likely involved in char formation, preventing them from fully transitioning into the gas phase during decomposition. Further for EV-7 and EV-8 the release of phosphorus species could be observed: PO^+ (*m/z*: 47), HPO^+ (*m/z*: 48), PO_2^+ (*m/z*: 63) and HPO_2^+ (*m/z*: 64). The formation of these fragments confirms the activity in the gas phase by acting as radical scavenger and flame inhibition. During the burning process the release of PO- and PO_2- radicals leads to a recombination with the hydrogen and hydroxyl radicals thereby interrupting the chain reaction by flame inhibition [57].

The intensity of the indicators for the volatile phosphorus species is increased for EV-8 in comparison to EV-7. This supports the assumption of a stronger gas phase activity of Exolit® EP 360 which is also observed during the cone calorimeter test. Regarding the flame retardant mechanism for Polyphlox® 3742 in EV-7 a dual mechanism with activity in the gas phase due to the release of PO- and PO_2- radicals and activity in the condensed phase due to the increased residue is proposed. Regarding the Exolit® EP 360 in EV-8 a prevalent mechanism in the gas phase due to the strong release of PO- and PO_2-radicals is proposed.

3.3. Stress relaxation and reprocessability

The softening observed during the glass transition, see chapter *3.2* is attributed to the increased free volume of polymer chains when heated beyond the T_g. As heating continues, the materials not only soften but also exhibit fluidity. In contrast, conventional epoxy thermosets do not become fluid upon heating due to their highly cross-linked network structure, which is stabilized by strong bonds and limits the mobility of the polymer chains [93]. Consequently, fully cross-linked thermoset materials lose their recyclability because they form a permanent network structure. However, the incorporation of the associative dynamic covalent disulfide bonds enables reprocessability which was studied by time- and temperature-dependent stress relaxation tests by DMA. 1 % strain was applied, and the relaxation modulus was monitored as function of time. Stress relaxation times of vitrimers can be describe by the Maxwell law. Based on the Maxwell's model for viscoelastic fluids, relaxation times were determined as the time needed for relaxing 63 % of the initial stress,

$$\frac{G_t}{G_0} = e^{\left(\frac{-t}{\tau}\right)}$$

where $\frac{G_t}{G_0}$ is the normalized relaxation modulus, and τ is the relaxation time (s) [94–96].

For conventional epoxy thermosets, the relaxation modulus does not comply the Maxwell law. The EVs studied in this work follow the Maxwell law though. The plotted $\frac{G_t}{G_0}$ against the time is shown in the supporting information for EV-0, EV-7 and EV-8 at temperatures between 150 °C and 210 °C for 15 minutes (Fig S4 (a), (b) and (c)). The EVs show relaxation times > 15 min at 140 °C but for temperatures ≥ 150 °C relaxation times of < 15 min were observed. The relaxation times clearly decreased with increasing temperatures. This could indicate an acceleration in the kinetics of the disulfide exchange reaction [95]. The flame retardants further do not interfere with the exchange reaction and the samples still exhibit characteristic vitrimeric behavior.

The temperature dependence of the relaxation time can be described using the Arrhenius law:

$$\tau(T) = \tau_0 e^{\left(\frac{E_a}{RT}\right)}$$

where E_a is the activation energy (J•mol^{-1}), and R is the ideal gas constant (J•mol^{-1}•K^{-1}).

The activation energy in vitrimers refers to the amount of energy required to activate the exchange reaction between the dynamic bonds resulting in a reconfiguration of the polymeric network of the material [43]. Under certain temperature conditions these bonds will rearrange and change the internal structure while maintaining their structural integrity.

The choice between lower or higher activation energy in vitrimers

Table 7
Relaxation times (τ), determined from the stress relaxation curves, and activation energies E_a calculated from the slope of the Arrhenius plot of EV-0, EV-7 and EV-8.

Sample	τ (s) at 200 °C	E_a / kJ•mol^{-1}
EV-0	22	130
EV-7	18	130
EV-8	21	138

depends on the application. For applications where reconfiguration, repair or recycling at low temperatures is required, a lower activation energy is preferable. However, for applications where structural stability is required at normal operating temperatures, a higher activation energy is more appropriate. Therefore, the balance between processability and thermal stability is crucial in determining an appropriate activation energy.

The activation energies calculated from the slopes of the linear fitting of ln(τ) against the inverse temperature (shown in the supporting information Fig S4 (d)), and the relaxation time at 200 °C determined from the stress relaxation curves for EV-0, EV-7 and EV-8 are presented in Table 7. At 200 °C, similar relaxation times were determined for EV-0, EV-7 and EV-8, between 18 s and 22 s.

EV-0 without FR shows an activation energy of 130 kJ•mol^{-1}. EV-7 shows the same value as EV-0. For EV-8 an activation energy of 138 kJ•mol^{-1} was calculated, demonstrating a slightly higher E_a. Nevertheless, the addition of flame retardants to the epoxy formulation did not significantly modify the activation energy.

It is therefore demonstrated that the incorporation of flame retardants in has not impeded the dynamism of the chemical structure, necessary for their processability, and still maintains structural stability.

3.4. Thermal, mechanical and flame retardant properties after recycling

After a mechanical recycling process of EV-0, EV-7 and EV-8 including grinding the material and hot pressing (see Fig. 9), the thermal, mechanical and flame retardant properties were analyzed again. The results are shown in Table 8.

With an isothermal TGA (see Fig. S5) the mass loss at 200 °C under air of EV-0, EV-7 and EV-8 for 30 min was analyzed to proof that the vitrimers do not start to decompose during the hot pressing. The mass loss of all samples is < 1.5 wt%.

The glass transition temperature decreased for rEV-0 slightly from 125 °C to 117 °C. For the flame retardant rEVs, rEV-7 and rEV-8, the T_g decreased as well to 111 °C and 110 °C. It is assumed, that during comminution covalent bonds are broken, which cannot be reformed by the exchange of disulfide bonds. This leads to a decrease in network density, resulting in a lower glass transition temperature and reduced thermal stability.

The LOI values for rEV-0 and rEV-7 remain at about 21 %O_2 and 29 %O_2. The LOI of rEV-8 decreased by 5 %O_2 from 38.5 %O_2 to 33.5 %O_2. However, the LOI value of rEV-8 is still significantly higher than the LOI values of rEV-0 and rEV-7.

The UL-94 classifications of all three recycled EVs remain unchanged. Both, rEV-7 and rEV-8 with phosphorus flame retardant reach the high V-0 classification. However, an increase of the after burning times is observed during UL-94 tests for these materials. Pictures of the UL-94 vertical burning tests of rEV-0 in comparison to rEV-8 are shown in Fig. 10.

To determine the influence of the reprocessability on the mechanical properties, tensile tests of the initial and recycled plates were performed. The modulus and tensile strength results of each formulation before (a) and after recycling (b) are compared in Fig. 11 (see also supporting information Table S1).

On the one hand, the modulus of the initial EVs was increased from 2209 MPa of EV-0 to 2470 MPa for EV-8 and 3476 MPa of EV-7. Presumably the modulus increases due to the novolac backbone of the Polyphlox® 3742. On the other hand, the tensile strength is somewhat affected by the FRs, decreasing from 85 MPa for EV-0 to 65 MPa for EV-7 while increasing up to 96 MPa for EV-8.

The Young's modulus in the recycled materials is either maintained or increased, suggesting that some of the ground resin may be acting as a filler, supporting part of the applied stress and reducing the deformation of the matrix. The tensile strength of rEV-0, rEV-7 and rEV-8 is reduced from the initial value. However, it recovers by 73 % for EV-0, 77 % for EV-7 and 75 % for EV-8 respectively. The probable reduction of the network density due to the comminution of the material also results in a decrease of the mechanical properties.

On the other hand, the dispersion of the mechanical properties of the recycled materials is noticeable, if part of the ground resin acts as a filler, the concentration and dispersion of these resin particles would also affect the homogeneity of the material.

In conclusion, the second-generation EVs show excellent flame retardant properties and a tensile strength higher than 70 %.

4. Conclusions

In this work, commercially available chemicals and FRs were used to successfully produce flame retardant, reprocessable epoxy vitrimers based on bisphenol A diglycidylether (DGEBA) and 4-amionphenyl disulfide (4-AFD). Different types of aliphatic, cycloaliphatic and

Table 8
Thermal and flame retardant properties of EV-0, EV-7 and EV-8 initial and recycled material.

Sample	T_g / °C	TGA		LOI / % O_2	UL-94
		$T_{2\ \%\ mass\ loss}$ / %	Residue (1000 °C) / %		
EV-0	125	274	13.6	20.9 ± 0.4	n.c.
rEV-0	117	265	12.7	21.3 ± 0.7	n.c.
EV-7	116	277	22.4	29.0 ± 0.4	V-0
rEV-7	111	263	20.7	29.3 ± 0.5	V-0
EV-8	113	273	19.5	38.5 ± 0.4	V-0
rEV-8	110	266	19.1	33.5 ± 0.4	V-0

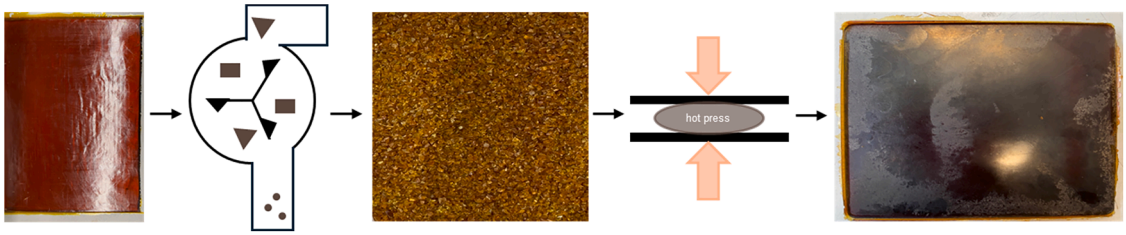

Fig. 9. Flow chart of the reprocessing used for the EVs.

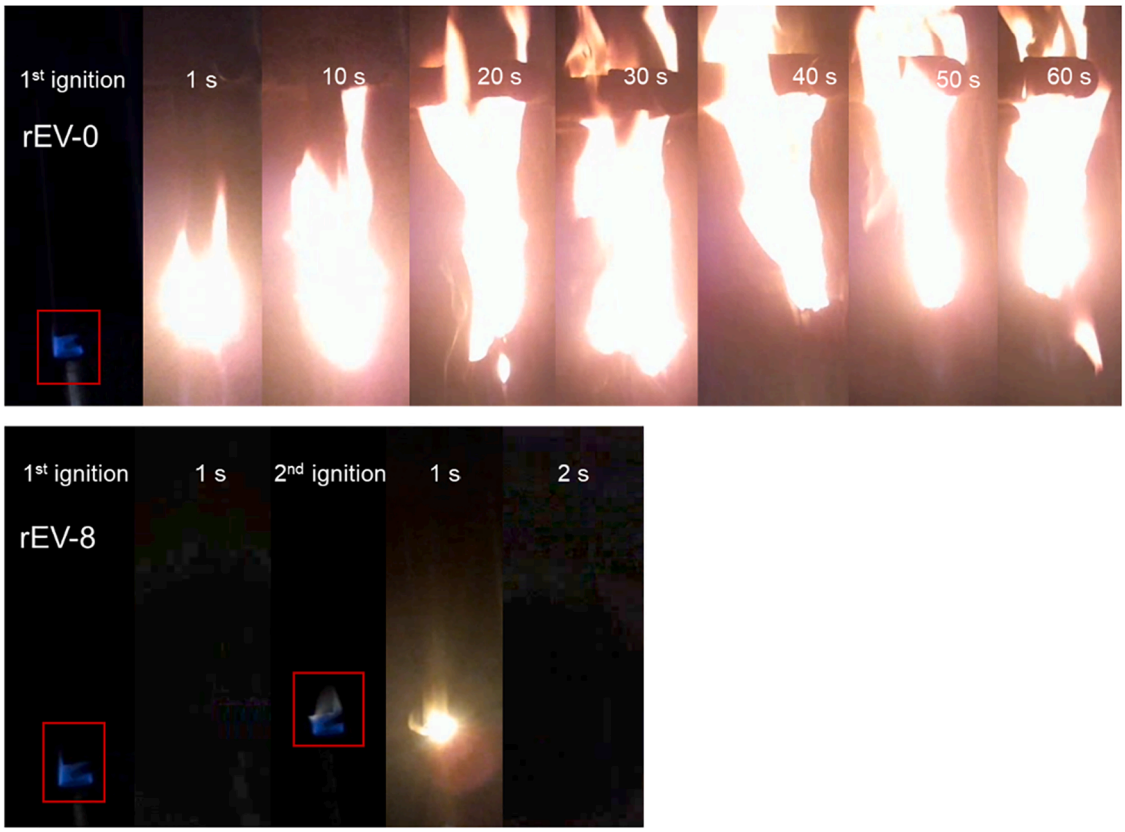

Fig. 10. Illustration of the flame retardant performance of the flame retardant free rEV-0 in comparison to the flame retardant rEV-8 during UL-94 test.

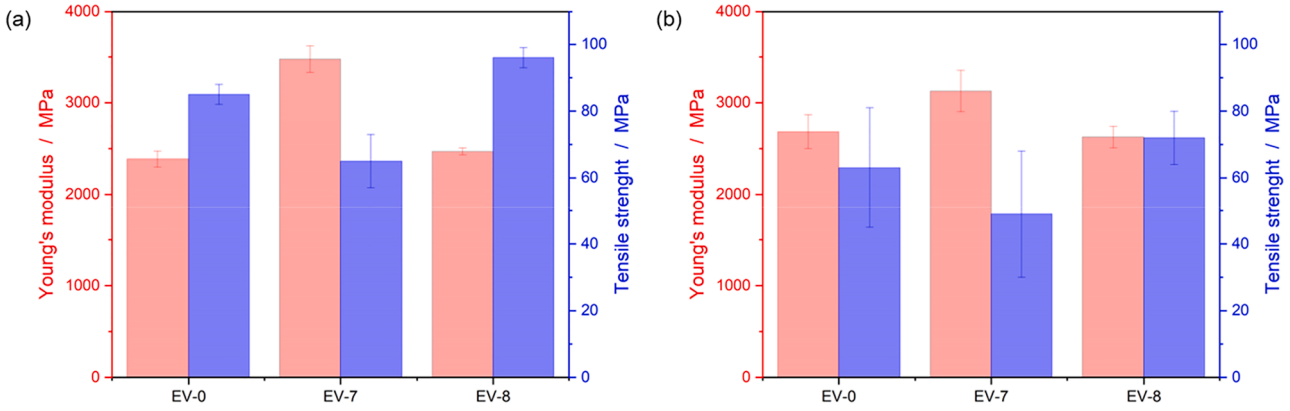

Fig. 11. Young's modulus and tensile strengths of (a) initial EVs and (b) reprocessed EVs.

naphthalene-based resins were added to investigate the influence of the aliphatic-aromatic ration on the thermal properties and flammability. Aliphatic resins decrease the glass transition temperature form EV-0 of 125 °C to 100 °C. Naphthalene-based resin increases the T_g to 139 °C. The flammability was not sufficiently improved. Modifying the epoxy resin system alone does not provide sufficient improvements regarding flammability. This clearly indicates the need of flame retardant solutions for this type of EV if it is to be used in applications with flame retardant requirements such as the transportation or electronic sector.

Phosphorous-based flame retardants of different oxidation states of the phosphorus incorporated with 1.5 wt% phosphorus in EV-0 were studied. All EVs show similar T_g values and similar thermal stability compared to EV-0. In the flammability test LOI and UL-94 tests, gas phase active phosphinates show highest improvement regarding the flame retardancy. The high UL-94 V-0 classification was reached for EV-6, EV-7 and EV-8 containing Exolit® OP 930, Polyphlox® 3742 and Exolit® EP 360. The highest LOI was achieved by EV-8 with 38.5 %O_2. The reactive flame retardants of EV-7 and EV-8 offer advantage in terms of safety and sustainability as the phosphorus compound is covalently bond to the vitrimer network. In comparison to EV-0, both EVs containing the reactive flame retardants show a reduction in PHRR by 43 % and 39 % respectively and MAHRE values of about 273 kW•m^{-2}. However, smoke release is increased by the flame retardants. MAHRE as well as smoke release are currently too high for typical applications in the transportation sector. However, a significant reduction in the values is expected if the EVs are used in fiber-reinforced composites which corresponds to a common application target for this type of material.

The dynamism and reprocessability of the EVs was studied by dynamic mechanical analysis. The disulfide exchange reaction is not disrupted by the addition of flame retardants. The activation energies for

the disulfide exchange reaction calculated by the Arrhenius law remains.

The second-generation materials obtained by a mechanical recycling process show the same excellent flame retardant properties and show a tensile strength of higher than 70 % in comparison to the first-generation materials.

The EV materials presented here show the potential to be a sustainable alternative for epoxy composites e.g., in the transportation and electronic sector. The corresponding EV composites are part of further investigations.

CRediT authorship contribution statement

Valeria Berner: Writing – original draft, Visualization, Validation, Methodology, Investigation, Formal analysis, Data curation, Conceptualization. **Arrate Huegun:** Writing – review & editing, Visualization, Validation, Methodology, Investigation, Formal analysis, Data curation, Conceptualization. **Larissa Hammer:** Writing – review & editing. **Anna Maria Cristadoro:** Writing – review & editing, Supervision, Resources, Project administration, Funding acquisition. **Carl-Christoph Höhne:** Writing – review & editing, Supervision, Resources, Project administration, Funding acquisition.

Declaration of competing interest

The authors declare the following financial interests/personal relationships which may be considered as potential competing interests:

Valeria Berner reports financial support was provided by Fraunhofer Institute for Chemical Technology ICT. If there are other authors, they declare that they have no known competing financial interests or personal relationships that could have appeared to influence the work reported in this paper

Acknowledgments

The authors would like to thank their colleagues from Fraunhofer ICT, Pfinztal: Beatrice Tübke, Yvonne Kasimir, Eyleen Napoli, Kristin Bergmann, Wenka Schweikert and Stefan Müller and from Fraunhofer LBF Katrin Markus for analytical support. This project has received the funding from the European Union's Horizon Europe research and innovation program under grant no. 101057901. Views and opinions expressed are however those of the authors only and do not necessarily reflect those of the European Union. Neither the European Union nor the granting authority can be held responsible for them.

Supplementary materials

Supplementary material associated with this article can be found, in the online version, at doi:10.1016/j.polymdegradstab.2024.111145.

Data availability

Data will be made available on request.

References

[1] P. Mohan, A Critical Review: The Modification, Properties, and Applications of Epoxy Resins, Polym. Plast. Technol. Eng. 52 (2) (2013) 107–125, https://doi.org/10.1080/03602559.2012.727057.
[2] F.L. Jin, X. Li, S.J. Park, Synthesis and application of epoxy resins: A review, Journal of Industrial and Engineering Chemistry 29 (2015) 1–11, https://doi.org/10.1016/j.jiec.2015.03.026.
[3] Y. Wen, et al., Advances on Thermally Conductive Epoxy-Based Composites as Electronic Packaging Underfill Materials-A Review, Advanced Materials 34 (52) (2022) e2201023, https://doi.org/10.1002/adma.202201023.
[4] R. Auvergne, S. Caillol, G. David, B. Boutevin, J.P. Pascault, Biobased thermosetting epoxy: present and future, Chem. Rev. 114 (2) (2014) 1082–1115, https://doi.org/10.1021/cr3001274.
[5] A. Wazeer, A. Das, C. Abeykoon, A. Sinha, A. Karmakar, Composites for electric vehicles and automotive sector: A review, Green Energy and Intelligent Transportation 2 (1) (2023) 100043, https://doi.org/10.1016/j.geits.2022.100043.
[6] B. Bilyeu, W. Brostow, K.P. Menard, Epoxy thermosets and their applications I: chemical structures and applications, Journal of Materials Education (21) (1999) 281–286 [Online]. Available, https://lapom.unt.edu/sites/default/files/epoxyjme1.pdf.
[7] J.C. Capricho, B. Fox, N. Hameed, Multifunctionality in Epoxy Resins, Polymer Reviews 60 (1) (2020) 1–41, https://doi.org/10.1080/15583724.2019.1650063.
[8] F.L. Jin, S.Y. Lee, S.J. Park, Polymer matrices for carbon fiber-reinforced polymer composites, Carbon letters 14 (2) (2013) 76–88, https://doi.org/10.5714/cl.2013.14.2.076.
[9] W. Post, A. Susa, R. Blaauw, K. Molenveld, R.J.I. Knoop, A Review on the Potential and Limitations of Recyclable Thermosets for Structural Applications, Polymer Reviews 60 (2) (2020) 359–388, https://doi.org/10.1080/15583724.2019.1673406.
[10] M.Y. Khalid, Z.U. Arif, W. Ahmed, H. Arshad, Recent trends in recycling and reusing techniques of different plastic polymers and their composite materials, Sustainable Materials and Technologies 31 (2022) e00382, https://doi.org/10.1016/j.susmat.2021.e00382.
[11] G. Oliveux, L.O. Dandy, G.A. Leeke, Current status of recycling of fibre reinforced polymers: Review of technologies, reuse and resulting properties, Prog. Mater. Sci. 72 (2015) 61–99, https://doi.org/10.1016/j.pmatsci.2015.01.004.
[12] S. Ma, D.C. Webster, Degradable thermosets based on labile bonds or linkages: A review, Prog. Polym. Sci. 76 (2018) 65–110, https://doi.org/10.1016/j.progpolymsci.2017.07.008.
[13] J.H. Chen, X.P. An, Y.D. Li, M. Wang, J.B. Zeng, Reprocessible Epoxy Networks with Tunable Physical Properties: Synthesis, Stress Relaxation and Recyclability, in En;en, Chinese Journal of Polymer Science 36 (5) (2018) 641–648, https://doi.org/10.1007/s10118-018-2027-9.
[14] W. Dang, M. Kubouchi, S. Yamamoto, H. Sembokuya, K. Tsuda, An approach to chemical recycling of epoxy resin cured with amine using nitric acid, Polymer. (Guildf) 43 (10) (2002) 2953–2958, https://doi.org/10.1016/S0032-3861(02)00100-3.
[15] M. Guerre, C. Taplan, J.M. Winne, F.E. Du Prez, Vitrimers: directing chemical reactivity to control material properties, Chem. Sci. 11 (19) (2020) 4855–4870, https://doi.org/10.1039/D0SC01069C.
[16] C.N. Bowman, C.J. Kloxin, Covalent adaptable networks: reversible bond structures incorporated in polymer networks, Angewandte Chemie International Edition 51 (18) (2012) 4272–4274, https://doi.org/10.1002/anie.201200708.
[17] C. Bowman, F.Du Prez, J. Kalow, Introduction to chemistry for covalent adaptable networks, Polym. Chem. 11 (33) (2020) 5295–5296, https://doi.org/10.1039/D0PY90102D.
[18] C.J. Kloxin, C.N. Bowman, Covalent adaptable networks: smart, reconfigurable and responsive network systems, Chem. Soc. Rev. 42 (17) (2013) 7161–7173, https://doi.org/10.1039/C3CS60046G.
[19] L. Hammer, N.J. van Zee, R. Nicolaÿ, Dually Crosslinked Polymer Networks Incorporating Dynamic Covalent Bonds, Polymers. (Basel) 13 (3) (2021), https://doi.org/10.3390/polym13030396, 396.
[20] C.J. Kloxin, T.F. Scott, B.J. Adzima, C.N. Bowman, Covalent Adaptable Networks (CANs): A Unique Paradigm in Crosslinked Polymers, Macromolecules. 43 (6) (2010) 2643–2653, https://doi.org/10.1021/ma902596s.
[21] J.M. Winne, L. Leibler, F.E. Du Prez, Dynamic covalent chemistry in polymer networks: a mechanistic perspective, Polym. Chem. 10 (45) (2019) 6091–6108, https://doi.org/10.1039/C9PY01260E.
[22] D. Montarnal, M. Capelot, F. Tournilhac, L. Leibler, Silica-like malleable materials from permanent organic networks, Science 334 (6058) (2011) 965–968, https://doi.org/10.1126/science.1212648.
[23] B.R. Elling, W.R. Dichtel, Reprocessable Cross-Linked Polymer Networks: Are Associative Exchange Mechanisms Desirable? ACS. Cent. Sci. 6 (9) (2020) 1488–1496, https://doi.org/10.1021/acscentsci.0c00567.
[24] B. Krishnakumar, R.P. Sanka, W.H. Binder, V. Parthasarthy, S. Rana, N. Karak, Vitrimers: Associative dynamic covalent adaptive networks in thermoset polymers, Chemical Engineering Journal 385 (2020) 123820, https://doi.org/10.1016/j.cej.2019.123820.
[25] D. Berne, et al., Catalyst-Free Epoxy Vitrimers Based on Transesterification Internally Activated by an α–CF 3 Group, Macromolecules. 55 (5) (2022) 1669–1679, https://doi.org/10.1021/acs.macromol.1c02538.
[26] J. Han, T. Liu, C. Hao, S. Zhang, B. Guo, J. Zhang, A Catalyst-Free Epoxy Vitrimer System Based on Multifunctional Hyperbranched Polymer, Macromolecules. 51 (17) (2018) 6789–6799, https://doi.org/10.1021/acs.macromol.8b01424.
[27] F. Cuminet, et al., Catalyst-free transesterification vitrimers: activation via α-difluoroesters, Polym. Chem. 13 (18) (2022) 2651–2658, https://doi.org/10.1039/D2PY00124A.
[28] T. Liu, B. Zhao, J. Zhang, Recent development of repairable, malleable and recyclable thermosetting polymers through dynamic transesterification, Polymer. (Guildf) 194 (2020) 122392, https://doi.org/10.1016/j.polymer.2020.122392.
[29] R. Hajj, A. Duval, S. Dhers, L. Avérous, Network Design to Control Polyimine Vitrimer Properties: Physical Versus Chemical Approach, Macromolecules. 53 (10) (2020) 3796–3805, https://doi.org/10.1021/acs.macromol.0c00453.
[30] X. Liu, L. Liang, M. Lu, X. Song, H. Liu, G. Chen, Water-resistant bio-based vitrimers based on dynamic imine bonds: Self-healability, remodelability and ecofriendly recyclability, Polymer. (Guildf) 210 (2020) 123030, https://doi.org/10.1016/j.polymer.2020.123030.
[31] H. Memon, Y. Wei, L. Zhang, Q. Jiang, W. Liu, An imine-containing epoxy vitrimer with versatile recyclability and its application in fully recyclable carbon fiber

reinforced composites, Compos. Sci. Technol. 199 (2020) 108314, https://doi.org/10.1016/j.compscitech.2020.108314.
[32] S. Zhao, M.M. Abu-Omar, Recyclable and Malleable Epoxy Thermoset Bearing Aromatic Imine Bonds, Macromolecules. 51 (23) (2018) 9816–9824, https://doi.org/10.1021/acs.macromol.8b01976.
[33] D.J. Fortman, J.P. Brutman, C.J. Cramer, M.A. Hillmyer, W.R. Dichtel, Mechanically activated, catalyst-free polyhydroxyurethane vitrimers, J. Am. Chem. Soc. 137 (44) (2015) 14019–14022, https://doi.org/10.1021/jacs.5b08084.
[34] P. Yan, et al., Multifunctional polyurethane-vitrimers completely based on transcarbamoylation of carbamates: thermally-induced dual-shape memory effect and self-welding, RSC. Adv. 7 (43) (2017) 26858–26866, https://doi.org/10.1039/C7RA01711A.
[35] T. Debsharma, V. Amfilochiou, A.A. Wróblewska, I. de Baere, W. van Paepegem, F. E. Du Prez, Fast Dynamic Siloxane Exchange Mechanism for Reshapable Vitrimer Composites, J. Am. Chem. Soc. 144 (27) (2022) 12280–12289, https://doi.org/10.1021/jacs.2c03518.
[36] X. Wu, X. Yang, R. Yu, X.J. Zhao, Y. Zhang, W. Huang, A facile access to stiff epoxy vitrimers with excellent mechanical properties via siloxane equilibration, Journal of Materials Chemistry A 6 (22) (2018) 10184–10188, https://doi.org/10.1039/C8TA02102C.
[37] Q. Liu, L. Jiang, Y. Zhao, Y. Wang, J. Lei, Reprocessable and Shape Memory Thermosetting Epoxy Resins Based on Silyl Ether Equilibration, Macromol. Chem. Phys. (2019) 1900149, https://doi.org/10.1002/macp.201900149.
[38] N. Tratnik, N.R. Tanguy, N. Yan, Recyclable, self-strengthening starch-based epoxy vitrimer facilitated by exchangeable disulfide bonds, Chemical Engineering Journal 451 (2023) 138610, https://doi.org/10.1016/j.cej.2022.138610.
[39] F. Ji, X. Liu, D. Sheng, Y. Yang, Epoxy-vitrimer composites based on exchangeable aromatic disulfide bonds: Reprocessibility, adhesive, multi-shape memory effect, Polymer. (Guildf) 197 (2020) 122514, https://doi.org/10.1016/j.polymer.2020.122514.
[40] C. Luo, et al., Cost-efficient and recyclable epoxy vitrimer composite with low initial viscosity based on exchangeable disulfide crosslinks, Polym. Test. 113 (2022) 107670, https://doi.org/10.1016/j.polymertesting.2022.107670.
[41] B. Li, G. Zhu, Y. Hao, T. Ren, An investigation on the performance of epoxy vitrimers based on disulfide bond, J. Appl. Polym. Sci. 139 (5) (2022) 51589, https://doi.org/10.1002/app.51589.
[42] H. Si, et al., Rapidly reprocessable, degradable epoxy vitrimer and recyclable carbon fiber reinforced thermoset composites relied on high contents of exchangeable aromatic disulfide crosslinks, Composites, Part B 199 (2020) 108278, https://doi.org/10.1016/j.compositesb.2020.108278.
[43] I. Azcune, A. Huegun, A. Ruiz de Luzuriaga, E. Saiz, A. Rekondo, The effect of matrix on shape properties of aromatic disulfide based epoxy vitrimers, Eur. Polym. J. 148 (2021) 110362, https://doi.org/10.1016/j.eurpolymj.2021.110362.
[44] I. Azcune, E. Elorza, A. Ruiz de Luzuriaga, A. Huegun, A. Rekondo, H.J. Grande, Analysis of the Effect of Network Structure and Disulfide Concentration on Vitrimer Properties, Polymers. (Basel) 15 (20) (2023), https://doi.org/10.3390/polym15204123.
[45] A. Ruiz de Luzuriaga, et al., Epoxy resin with exchangeable disulfide crosslinks to obtain reprocessable, repairable and recyclable fiber-reinforced thermoset composites, Mater. Horiz. 3 (3) (2016) 241–247, https://doi.org/10.1039/C6MH00029K.
[46] A. Ruiz de Luzuriaga, G. Solera, I. Azcarate-Ascasua, V. Boucher, H.J. Grande, A. Rekondo, Chemical control of the aromatic disulfide exchange kinetics for tailor-made epoxy vitrimers, Polymer. (Guildf) 239 (2022) 124457, https://doi.org/10.1016/j.polymer.2021.124457.
[47] I. Azcune, I. Odriozola, Aromatic disulfide crosslinks in polymer systems: Self-healing, reprocessability, recyclability and more, Eur. Polym. J. 84 (2016) 147–160, https://doi.org/10.1016/j.eurpolymj.2016.09.023.
[48] A. Rekondo, R. Martin, A. Ruiz de Luzuriaga, G. Cabañero, H.J. Grande, I. Odriozola, Catalyst-free room-temperature self-healing elastomers based on aromatic disulfide metathesis, Mater. Horiz. 1 (2) (2014) 237–240, https://doi.org/10.1039/C3MH00061C.
[49] J.M. Matxain, J.M. Asua, F. Ruipérez, Design of new disulfide-based organic compounds for the improvement of self-healing materials, Physical Chemistry Chemical Physics 18 (3) (2016) 1758–1770, https://doi.org/10.1039/C5CP06660C.
[50] A. Takahashi, T. Ohishi, R. Goseki, H. Otsuka, Degradable epoxy resins prepared from diepoxide monomer with dynamic covalent disulfide linkage, Polymer. (Guildf) 82 (2016) 319–326, https://doi.org/10.1016/j.polymer.2015.11.057.
[51] D. Martinez-Diaz, A. Cortés, A. Jiménez-Suárez, S.G. Prolongo, Hardener Isomerism and Content of Dynamic Disulfide Bond Effect on Chemical Recycling of Epoxy Networks, ACS. Appl. Polym. Mater. 4 (7) (2022) 5068–5076, https://doi.org/10.1021/acsapm.2c00598.
[52] S.Y. Lu, I. Hamerton, Recent developments in the chemistry of halogen-free flame retardant polymers, Prog. Polym. Sci. 27 (8) (2002) 1661–1712, https://doi.org/10.1016/S0079-6700(02)00018-7.
[53] M.M. Velencoso, A. Battig, J.C. Markwart, B. Schartel, F.R. Wurm, Molekulare Brandbekämpfung – wie moderne Phosphorchemie zur Lösung der Flammschutzaufgabe beitragen kann, in de, Angewandte Chemie 130 (33) (2018) 10608–10626, https://doi.org/10.1002/ange.201711735.
[54] Z. Huang, et al., Enabling simultaneous reprocessability and fire protection via incorporation of phosphine oxide monomer in epoxy vitrimer, J. Mater. Sci. Technol. 196 (2024) 224–236, https://doi.org/10.1016/j.jmst.2024.01.062.
[55] S. Bourbigot, M. Le Bras, Flame Retardant Plastics, in: J. Troitzsch (Ed.), Plastics Flammability handbook: Principles, regulations, testing, and Approval, 3rd ed., Hanser, München, 2013, pp. 133–172.
[56] P. Joseph, J.R. Ebdon, Phosphorus-Based Flame Retardants, in: C.A. Wilkie, A. B. Morgan (Eds.), Fire Retardancy of Polymeric Materials, 2nd ed., CRC Press, Boca Raton, 2010, pp. 107–128.
[57] B. Schartel, Phosphorus-based Flame Retardancy Mechanisms-Old Hat or a Starting Point for Future Development? Materials 3 (10) (2010) 4710–4745, https://doi.org/10.3390/ma3104710.
[58] U. Braun, et al., Influence of the oxidation state of phosphorus on the decomposition and fire behaviour of flame-retarded epoxy resin composites, Polymer. (Guildf) 47 (26) (2006) 8495–8508, https://doi.org/10.1016/j.polymer.2006.10.022.
[59] U. Braun, B. Schartel, Flame Retardancy Mechanisms of Aluminium Phosphinate in Combination with Melamine Cyanurate in Glass-Fibre-Reinforced Poly(1,4-butylene terephthalate), Macromol. Mater. Eng. 293 (3) (2008) 206–217, https://doi.org/10.1002/mame.200700330.
[60] S. Rabe, Y. Chuenban, B. Schartel, Exploring the Modes of Action of Phosphorus-Based Flame Retardants in Polymeric Systems, Materials 10 (5) (2017), https://doi.org/10.3390/ma10050455.
[61] J. Wagner, P. Deglmann, S. Fuchs, M. Ciesielski, C.A. Fleckenstein, M. Döring, A flame retardant synergism of organic disulfides and phosphorous compounds, Polym. Degrad. Stab. 129 (2016) 63–76, https://doi.org/10.1016/j.polymdegradstab.2016.03.023.
[62] W. Pawelec, et al., Disulfides – Effective radical generators for flame retardancy of polypropylene, Polym. Degrad. Stab. 110 (2014) 447–456, https://doi.org/10.1016/j.polymdegradstab.2014.09.013.
[63] C.C. Höhne, C. Posern, U. Böhme, F. Eichler, E. Kroke, Dithiocyanurates and thiocyamelurates: Thermal thiyl radical generators as flame retardants in polypropylene, Polym. Degrad. Stab. 166 (2019) 17–30, https://doi.org/10.1016/j.polymdegradstab.2019.05.004.
[64] M. Abdur Rashid, W. Liu, Y. Wei, Q. Jiang, Review of reversible dynamic bonds containing intrinsically flame retardant biomass thermosets, Eur. Polym. J. 173 (2022) 111263, https://doi.org/10.1016/j.eurpolymj.2022.111263.
[65] W.Wu Klingler, et al., Recyclable flame retardant phosphonated epoxy based thermosets enabled via a reactive approach, Chemical Engineering Journal 466 (2023) 143051, https://doi.org/10.1016/j.cej.2023.143051.
[66] X. Li, J. Zhang, L. Zhang, A. Ruiz de Luzuriaga, A. Rekondo, D.Y. Wang, Recyclable flame-retardant epoxy composites based on disulfide bonds: Flammability and recyclability, Composites Communications 25 (2021) 100754, https://doi.org/10.1016/j.coco.2021.100754.
[67] W. Yang, et al., Design of inherent fire retarding and degradable bio-based epoxy vitrimer with excellent self-healing and mechanical reprocessability, Compos. Sci. Technol. 230 (2022) 109776, https://doi.org/10.1016/j.compscitech.2022.109776.
[68] W.Wu Klingler, A. Bifulco, C. Polisi, Z. Huang, S. Gaan, Recyclable inherently flame-retardant thermosets: Chemistry, properties and applications, Composites Part B: Engineering 258 (2023) 110667, https://doi.org/10.1016/j.compositesb.2023.110667.
[69] S. Wang, S. Ma, Q. Li, W. Yuan, B. Wang, J. Zhu, Robust, Fire-Safe, Monomer-Recovery, Highly Malleable Thermosets from Renewable Bioresources, Macromolecules. 51 (20) (2018) 8001–8012, https://doi.org/10.1021/acs.macromol.8b01601.
[70] Y. Liu, et al., Phosphate-based covalent adaptable networks with recyclability and flame retardancy from bioresources, Eur. Polym. J. 144 (2021) 110236, https://doi.org/10.1016/j.eurpolymj.2020.110236.
[71] X. Luo, X.F. Liu, X.M. Ding, L. Chen, S.C. Chen, Y.Z. Wang, Effects of curing temperature on the structure and properties of epoxy resin-poly(ε-caprolactam) blends, Polymer. (Guildf) 228 (2021) 123940, https://doi.org/10.1016/j.polymer.2021.123940.
[72] R. Jian, P. Wang, L. Xia, X. Zheng, Effect of a novel P/N/S-containing reactive flame retardant on curing behavior, thermal and flame-retardant properties of epoxy resin, J. Anal. Appl. Pyrolysis. 127 (2017) 360–368, https://doi.org/10.1016/j.jaap.2017.07.014.
[73] M. Ou, et al., Co-curing preparation of flame retardant and smoke-suppressive epoxy resin with a novel phosphorus-containing ionic liquid, Chemosphere 311 (Pt 1) (2023) 137061, https://doi.org/10.1016/j.chemosphere.2022.137061.
[74] B.K. Kandola, B. Biswas, D. Price, A.R. Horrocks, Studies on the effect of different levels of toughener and flame retardants on thermal stability of epoxy resin, Polym. Degrad. Stab. 95 (2) (2010) 144–152, https://doi.org/10.1016/j.polymdegradstab.2009.11.040.
[75] J. Li, et al., Controlled Triphenylphosphine Reactivity for Epoxy Resin Cure by Transition-Metal β-Diketonates, Chemistry of Materials 34 (7) (2022) 3280–3300, https://doi.org/10.1021/acs.chemmater.2c00067.
[76] D. Aoki, S. Dogoshi, Y. Ito, K. Arimitsu, Thermal curing of epoxy resins at lower temperature using 4-(methylamino)pyridine derivatives as novel thermal latent curing agents, Journal of Polymer Science 62 (19) (2024) 4406–4415, https://doi.org/10.1002/pol.20240379.
[77] G. Socrates, Infrared and Raman characteristic Group frequencies: Tables and Charts, 3rd ed., John Wiley & Sons LTD, Chichester, 2015.
[78] N. Tudorachi, F. Mustata, Curing and thermal degradation of diglycidyl ether of bisphenol A epoxy resin crosslinked with natural hydroxy acids as environmentally friendly hardeners, Arab. J. Chem. 13 (1) (2020) 671–682, https://doi.org/10.1016/j.arabjc.2017.07.008.
[79] J.D. McCoy, et al., Cure mechanisms of diglycidyl ether of bisphenol A (DGEBA) epoxy with diethanolamine, Polymer. (Guildf) 105 (2016) 243–254, https://doi.org/10.1016/j.polymer.2016.10.028.
[80] A. Toldy, P. Niedermann, Á. Pomázi, G. Marosi, B. Szolnoki, Flame Retardancy of Carbon Fibre Reinforced Sorbitol Based Bioepoxy Composites with Phosphorus-

Containing Additives, Materials 10 (5) (2017) 467, https://doi.org/10.3390/ma10050467.
[81] Á. Pomázi, B. Szolnoki, A. Toldy, Flame Retardancy of Low-Viscosity Epoxy Resins and Their Carbon Fibre Reinforced Composites via a Combined Solid and Gas Phase Mechanism, Polymers. (Basel) 10 (10) (2018) 1081, https://doi.org/10.3390/polym10101081.
[82] R. Ménard, C. Negrell, L. Ferry, R. Sonnier, G. David, Synthesis of biobased phosphorus-containing flame retardants for epoxy thermosets comparison of additive and reactive approaches, Polym. Degrad. Stab. 120 (2015) 300–312, https://doi.org/10.1016/j.polymdegradstab.2015.07.015.
[83] S. Weerathaworn, A. Meyer, V. Abetz, Vitrimers based on block copolymers with diverse block sequences, Polymer. (Guildf) 308 (2024) 127311, https://doi.org/10.1016/j.polymer.2024.127311.
[84] S.V. Levchik, E.D. Weil, Thermal decomposition, combustion and flame-retardancy of epoxy resins—A review of the recent literature, Polym. Int. 53 (12) (2004) 1901–1929, https://doi.org/10.1002/pi.1473.
[85] M. Rakotomalala, S. Wagner, M. Döring, Recent Developments in Halogen Free Flame Retardants for Epoxy Resins for Electrical and Electronic Applications, Materials 3 (8) (2010) 4300–4327, https://doi.org/10.3390/ma3084300.
[86] W.Y. Chen, Y.Z. Wang, F.C. Chang, Thermal and Flame Retardation Properties of Melamine Phosphate-Modified Epoxy Resins, in En;en, Journal of Polymer Research 11 (2) (2004) 109–117, https://doi.org/10.1023/B:JPOL.0000031069.23622.bc.
[87] T. Mariappan, C.A. Wilkie, Flame retardant epoxy resin for electrical and electronic applications, Fire Mater. 38 (5) (2014) 588–598, https://doi.org/10.1002/fam.2199.
[88] P. Zheng, R. Wang, D. Wang, X. Peng, Y. Zhao, Q. Liu, A phosphorus-containing hyperbranched phthalocyanine flame retardant for epoxy resins, Sci. Rep. 11 (1) (2021) 17731, https://doi.org/10.1038/s41598-021-96927-y.
[89] P.M. Hergenrother, et al., Flame retardant aircraft epoxy resins containing phosphorus, Polymer. (Guildf) 46 (14) (2005) 5012–5024, https://doi.org/10.1016/j.polymer.2005.04.025.
[90] B. Zirnstein, W. Tabaka, D. Frasca, D. Schulze, B. Schartel, Graphene /hydrogenated acrylonitrile-butadiene rubber nanocomposites: Dispersion, curing, mechanical reinforcement, multifunctional filler, Polym. Test. 66 (2018) 268–279, https://doi.org/10.1016/j.polymertesting.2018.01.035.
[91] M. Häublein, K. Peter, G. Bakis, R. Mäkimieni, V. Altstädt, M. Möller, Investigation on the Flame Retardant Properties and Fracture Toughness of DOPO and Nano-SiO2 Modified Epoxy Novolac Resin and Evaluation of Its Combinational Effects, Materials 12 (9) (2019) 1528, https://doi.org/10.3390/ma12091528.
[92] C.D. Varganici, L. Rosu, A. Bifulco, D. Rosu, F. Mustata, S. Gaan, Recent advances in flame retardant epoxy systems from reactive DOPO–based phosphorus additives, Polym. Degrad. Stab. 202 (2022) 110020, https://doi.org/10.1016/j.polymdegradstab.2022.110020.
[93] R. Hardis, J.L. Jessop, F.E. Peters, M.R. Kessler, Cure kinetics characterization and monitoring of an epoxy resin using DSC, Raman spectroscopy, and DEA, Composites Part A: Applied Science and Manufacturing 49 (2013) 100–108, https://doi.org/10.1016/j.compositesa.2013.01.021.
[94] W. Zou, J. Dong, Y. Luo, Q. Zhao, T. Xie, Dynamic Covalent Polymer Networks: from Old Chemistry to Modern Day Innovations, Advanced Materials 29 (14) (2017), https://doi.org/10.1002/adma.201606100.
[95] H. Fang, W. Ye, Y. Ding, H.H. Winter, Rheology of the Critical Transition State of an Epoxy Vitrimer, Macromolecules. 53 (12) (2020) 4855–4862, https://doi.org/10.1021/acs.macromol.0c00843.
[96] A. Ruiz de Luzuriaga, N. Markaide, A.M. Salaberria, I. Azcune, A. Rekondo, H. J. Grande, Aero Grade Epoxy Vitrimer towards Commercialization, Polymers. (Basel) 14 (15) (2022) 3180, https://doi.org/10.3390/polym14153180.